Multichannel fiber optic Fabry-Perot nonscanning correlation demodulator

Ning Wang (王 宁)*, Yong Zhu (朱 永), Tiancheng Gong (龚天诚), Lihui Li (李丽慧), and Weimin Chen (陈伟民)

College of Opto-electronic Engineering, Chongqing University, Chongqing 400044, China

**Corresponding author: wn1983@163.com*

Received January 24, 2013; accepted April 3, 2013; posted online July 3, 2013

A multichannel fiber-optic Fabry-Perot (F-P) demodulator based on nonscanning correlation demodulation is proposed. The demodulator principle is analyzed, and the prototype of nonscanning correlation demodulation fiber-optic F-P demodulator is made and tested. The measurement range of the prototype is from 10 to 40 μm, the demodulation resolution is 8 nm, and its stability is 7 nm. This method provides a feasible solution, which guarantees the practicability of the fiber-optic F-P sensor network.

OCIS codes: 060.2370, 120.2230, 060.2300.

doi: 10.3788/COL201311.070601.

The fiber-optic Fabry-Perot (F-P) sensor in long-term remote sensing has small-volume, lightweight, low power-consumption, high-sensitivity, good-stability, and electromagnetic interference immunity features[1−3]. Therefore, a fiber-optic F-P sensor is regarded as an ideal candidate for special applications, such as in structural health monitoring of large-scale civil architecture[4−7].

System cost and sensor multiplex are two bottleneck problems in sensor development. In terms of structure, multiplex technology includes series, series-parallel, and parallel multiplexes[8,9]. Series multiplex needs only a single fiber-optic to realize distribution measurement in the structure, along with a few wires with a simple wire arrangement. However, apart from the relatively complicated series multiplex fabrication and demodulation algorithm, the cost is high and reliability and accuracy are low[10,11]. Meanwhile, parallel multiplex involves sensors that are independent of each other. Although the system is complicated and the cost is high, influence among sensors within the system is low and its stability is excellent[12]. Improving multiplex technology is an issue that requires an immediate solution to ensure the practicability of the fiber-optic F-P sensor network. Therefore, it is important to propose a novel multiplex method, which is highly accurate but low in cost.

Correlation demodulation does not require moving parts and expensive laser light source; thus, it has the capability to realize absolute cavity measurement. In addition, correlation demodulation is also widely used in fiber-optic F-P demodulation. A multichannel F-P demodulator based on nonscanning correlation demodulation is proposed in this letter (Fig. 1).

Firstly, the light was coupled into eight 1×2 couplers from a broadband light source by coupling lens, with each coupler connected to one F-P sensor. Eight sensors that passed through the channel were orderly switched, and the information of the F-P sensors was orderly coupled into the demodulation system. Hence, the multichannel F-P sensor information demodulation was achieved. The channel switch was irrelevant to the wavelength of light source, and the transmission of different wavelengths was accordant. The distribution of the fibers is shown in Fig. 1. Based on the demodulation system optical principle, the imaging size on the charge-coupled device (CCD) of each fiber is approximately 125 μm, and the maximum deviation among the fibers is 125 μm. Therefore, the 8-channel measurement is achieved effectively when the width of the CCD photosensitive surface is 200 μm. The channel number can be easily increased by changing the number of fiber and the optical system characteristics.

The principle of the correlation demodulator by considering the light source, which has Gaussian distribution in both spectrum and space, is shown as

$$I_{\rm out}(x) = {\rm e}^{-\frac{(x-x_{\rm p})^2}{B_x^2}} \cdot \int_{\lambda_{\min}}^{\lambda_{\max}} \frac{2R_1\left(1+\cos\frac{4\pi L}{\lambda}\right)}{1+R_1^2+2R_1\cos\frac{4\pi L}{\lambda}} \cdot \frac{(1-R_2)^2}{1+R_2^2-2R_2\cos\frac{4\pi x\tan\theta}{\lambda}} \cdot I_0(\lambda)\cdot {\rm e}^{-(\lambda-\lambda_{\rm p})^2/B_\lambda^2}{\rm d}\lambda, \tag{1}$$

where R_1 is the end face reflectivity of the fiber-optic F-P sensor, R_2 is the reflectivity of the Fizeau interferometer, B_λ is the half-width of the light source spectrum, λ is the current wavelength of the light sources, $\lambda_{\rm p}$ is the central wavelength of the light source, θ is the optical wedge angle, $I_0(\lambda)$ is the input light spectrum density and is ideally a constant, $I_0\,(\lambda)\cdot {\rm e}^{-(\lambda-\lambda_{\rm p})^2/B_\lambda^2}$ is the input light spectrum density by considering the Gaussian distribution in the spectrum, $I_{\rm out}$ is the output light intensity, L is the F-P cavity length, x is the optical wedge length equals the length of CCD, $x_{\rm p}$ is the center of the space distribution of the light source, and B_x is the half-width of Gaussian function decided by light source space

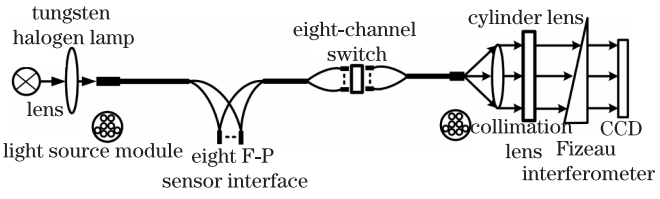

Fig. 1. Schematic of the multichannel F-P demodulator.

width. The intensity space distribution of the light source is considered as one dimensional because of the effect of the cylinder lens.

The relationship between optical wedge thickness and light intensity can be calculated using Eq. (1), as shown in Fig. 2. The optical wedge thickness with maximum light intensity is equal to the F-P cavity length; by comprehensive analysis, the system parameters R_1, R_2, and the optical wedge θ are 0.04°, 0.5°, and 0.01°, respectively.

The demodulator hardware system based on advanced RISC machines (ARM) and field-programmable gate array (FPGA) was designed in accordance with the system principle shown in Fig. 1. The multimode optical fiber was used in the system, and its numerical aperture was 0.22. The linear array CCD was TCD1304DG, which had 3648 effective pixels. Data on the cavity length of the F-P and its measurement information were obtained by calibration. The prototype is shown in Fig. 3.

The prototype can measure the indexes of pixels corresponding to the fiber-optic F-P sensor cavity length obtained through the calibrated formula. The result of the standard cavity length (15.383 μm) measured in this prototype is shown in Fig. 4.

Figure 4 shows the presence of low- and high-frequency noises in the original signal which make it difficult to obtain F-P cavity length. A signal correction algorithm is proposed, which effectively filters noise, highly improves the contrast ratio of signals, and achieves the precise measurement of the fiber-optic F-P sensor cavity length. The filtering result is shown in Fig. 5.

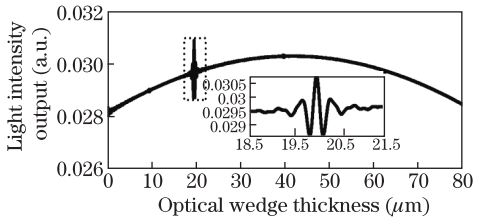

Fig. 2. Relationship between optical wedge thickness and light intensity output.

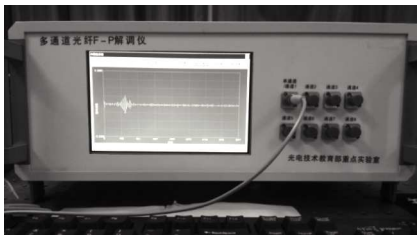

Fig. 3. Photograph of the experimental device.

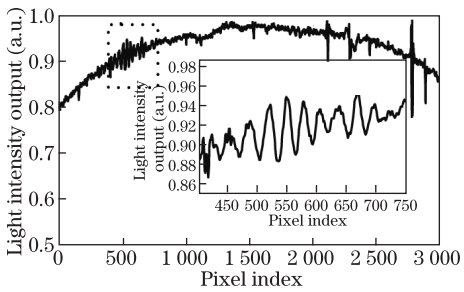

Fig. 4. Original signal.

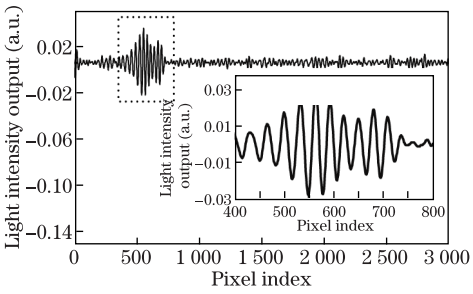

Fig. 5. Signal with processing.

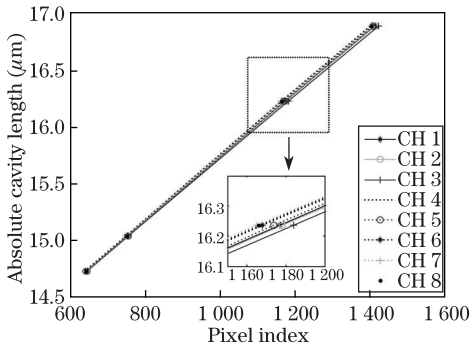

Fig. 6. Calibration results of the cavity length of each channel.

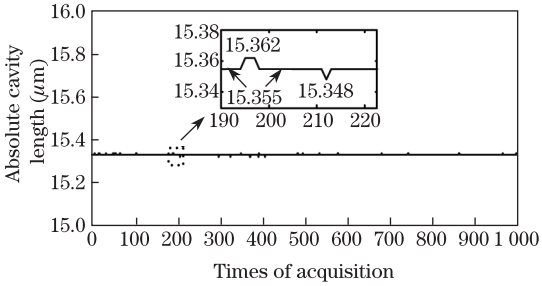

Fig. 7. Stability test of cavity length.

The calibration applies four standard F-P cavities, with cavity lengths of 14.732, 15.047, 16.236, and 16.898 μm, respectively. Figure 6 shows that the cavity calibration results of all channels are consistent with one another and in linear change. With reference to calibration, the measurement range of the prototype is from 10 to 40 μm, and the resolution is 8 nm.

The stability test was applied to each channel of the system. For example, channel 1 was tested continuously for 1 000 times in a condition where the four standard F-P cavities were stable. The results in Fig. 7 indicate that the maximum of the correlation function only deviates one image-sensitive element to the left or right side, that is, the measurement stability of this system is 7 nm.

The loading and unloading experiments of the single sensor on the constant strength beam were carried out to verify the demodulation accuracy of the prototype for the strain measurement. The residual error for the loading experiment was set to 2.8 nm and that for the unloading experiment was set to 3.4 nm. The experiment al results indicate that the prototype has good linearity and high measurement accuracy.

In conclusion, an 8-channel nonscanning fiber-optic F-P demodulator is designed based on the correlation demodulation principle. The theoretical model of the sys-

tem is established, and the optical parameters of the system are optimized. The measurement range of the prototype is from 10 to 40 μm, the resolution is 8 nm, and the stability is 7 nm. This prototype achieves the parallel multiplex of eight F-P sensors. Theoretically, 16-channel measurements can be achieved by changing the optical system. The effectuation of the 8-channel fiber-optic F-P demodulator provides a feasible solution for ensuring the practicability of the F-P sensors network. However, conducting further research on the system is still necessary. For example, the system requires a dynamic change in the F-P sensor to test the dynamic characteristics of the demodulator, which is a key topic in future research.

References

1. A. D. Kersey, M. A. Davis, H. J. Patrick, M. Le Blanc, K. P. Koo, C. G. Askins, M. A. Putnam, and E. J. Friebele, J. Lightwave Technol. **15,** 1442 (1997).
2. J. Zhang, H. Sun, and Q. Rong, Chin. Opt. Lett. **10,** 070607 (2012).
3. T. Zhao, Y. Gong, and Y. Rao, Chin. Opt. Lett. **9,** 050602 (2011).
4. J. H. Zhao, M. Z. Luo, Y. K. Shi, and J. L. Hua, in *Proceedings of the 12th International Conference on Inspection Appraisal Repairs and Maintenance of Structures* 1509 (2010).
5. L. Yan, W. Pan, and B. Luo, IEEE Sens. J. **11,** 1587 (2011).
6. C. W. Lai, Y. L. Lo, J. P. Yur, and C. H. Chuang, IEEE Sens. J. **12,** 827 (2012).
7. Y. Zhu, W. Chen, Y. Fu, and S. Huang, Proc. SPIE **6314,** 63140Y (2006).
8. W. H. Wang, X. S. Jiang, and Q. X. Yu, Opt. Commun. **285,** 3466 (2012).
9. Y. J. Rao, S. F. Yuan, X. K. Zeng, D. K. Lian, Y. Zhu, Y. P. Wang, S. L. Huang, and T. Y. Liu, Opt. Lasers Eng. **38,** 557 (2002).
10. O. C. Akkaya, O. Kilic, M. J. F. Digonnet, G. S. Kino, and O. Solgaard, in *Proceedings of IEEE Sensors Conference* 1148 (2010).
11. J. C. Xu, G. R. Pickrell, X. Wang, B. Wei, K. Yu, L. Cooper, and A. Wang, Proc. SPIE **5998,** 599809 (2005).
12. Y. J. Rao, J. Jiang, and C. X. Zhou, Sens. Actuat. **120,** 354 (2005).